SIMULATION ASPECTS OF PERFORMANCE AND EXPERIMENTAL PROCEDURES FOR A MICROACCELEROMETER

Georgeta IONASCU[1], Adriana SANDU[2], Lucian BOGATU[3], Constantin Daniel COMEAGA[4], Elena MANEA[5], Daniel BESNEA[6]

În lucrare este prezentat un studiu asupra comportamentului dinamic al structurii unui microaccelerometru piezorezistiv din siliciu, folosind metoda elementelor finite. Au fost determinate modurile de vibraţii (frecvenţele de rezonanţă) şi sensibilitatea. Sunt prezentate, de asemenea, rezultatele experimentale referitoare la fabricarea structurii microaccelerometrului şi testarea acesteia cu ajutorul analizorului de microsisteme MSA-500 (Polytec).

In this paper, a study on the dynamic behavior of the structure of a silicon piezoresistive microaccelerometer, by using FEM (Finite Element Method), is presented. The vibration modes (resonant frequencies) and sensitivity have been determined. The experimental results related to the fabrication process of the microaccelerometer structure and its testing on the MSA-500 Micro System Analyzer (Polytec) are also, presented

Keywords: micromechatronic device, silicon, accelerometer, FEM, performance

1. Introduction

Micro-Electro-Mechanical Systems (MEMS), also known as micromechatronic devices, integrate on the same chip (substrate) both miniaturized mechanical structures and microelectronics components. Acceleration sensors have been amongst the first successfully implemented MEMS products. Various MEMS accelerometers have been reported, made through bulk or surface micromachining (using crystalline anisotropy property of

[1] Prof., Dept. of Mechatronics and Precision Mechanics, University POLITEHNICA of Bucharest, ROMANIA, e-mail: ionascu_georgeta@yahoo.com
[2] Prof., Dept. of Strength of Materials, University POLITEHNICA of Bucharest, ROMANIA
[3] Lecturer, Dept. of Mechatronics and Precision Mechanics, University POLITEHNICA of Bucharest, ROMANIA
[4] Assoc. Prof., Dept. of Mechatronics and Precision Mechanics, University POLITEHNICA of Bucharest, ROMANIA
[5] PhD, National Institute for Research & Development in Microtechnology of Bucharest, ROMANIA
[6] Lecturer, Dept. of Mechatronics and Precision Mechanics, University POLITEHNICA of Bucharest, ROMANIA

silicon wafer or sacrificial layer technique, respectively) [1, 2], and employing different sensing schemes based on piezoresistive [3, 4, 5, 6], piezoelectric [7], capacitive [8, 9], or resonance [10] effect. The design is influenced by application, process facilities, yield and cost.

The performance of microaccelerometers [11, 12] can be achieved when the resonant frequency and the sensitivity requirements are fulfilled. The resonant frequency characterizes the bandwidth, as well as the physical sensitivity of the accelerometer. The accelerometer sensitivity is a function of the required magnitude of acceleration to be sensed and the method of sensing.

In this paper, a numerical model (FEM) of computation for the structure of a piezoresistive microaccelerometer has been developed. The FEM simulations were performed to determine the vibration modes (resonant frequencies), the location of piezoresistors and sensitivity, and to demonstrate decoupling of inertial force components on the three axes. The fabrication process of accelerometer structure by using MEMS technology (silicon bulk-micromachining) is, also, presented. In order to characterize the dynamic behavior and the geometry of accelerometer structure and to validate the numerical model of computation, the MSA-500 Micro System Analyzer has been used, with the non-contact measurement technologies of three-dimensional shape and motion in microstructures: Laser-Doppler Vibrometry (LDV) and White Light Interferometry (WLI).

2. Accelerometer structure

The sensor under study is a piezoresistive silicon microaccelerometer, conceived to detect acceleration in all the three directions. Its mechanical structure (figures 1a and 1b) consists of an inertial mass, symmetrically situated and suspended on a rim, using four micro-beams. The sensitive elements (piezoresistors) are diffused into the suspension arms, nearly the rim and the inertial mass, on perpendicular directions (Figs. 1a and 1c). The structure dimensions and materials are given in Fig. 2. The silicon substrate and two layers of silicon dioxide on its both sides, used as masks in the fabrication process, can be observed.

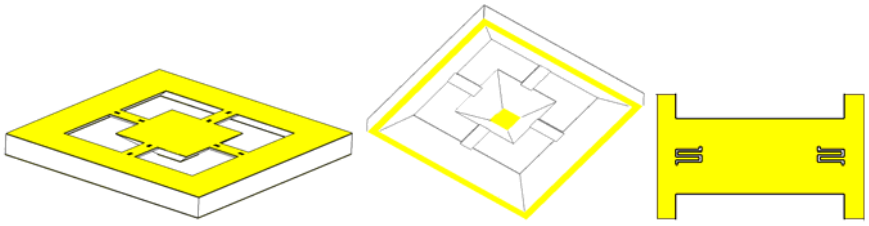

a) b) c)

Fig. 1. Views of accelerometer structure: front side (a), back side (b) and piezoresistors positioning in a detail (c).

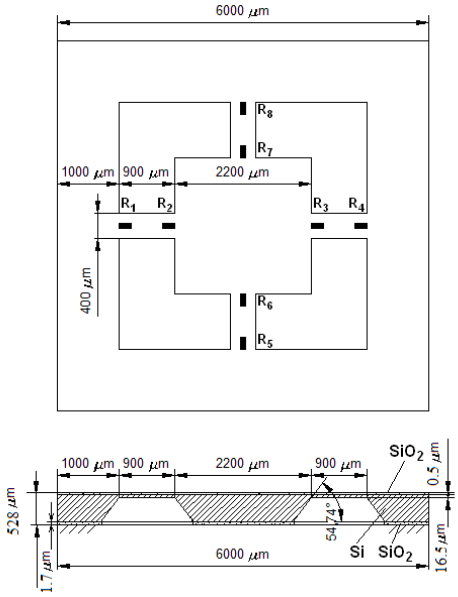

Fig. 2. Components and sizes of the analysed structure. Overall dimensions of piezoresistors: w_p (width)~70μm, l_p (length)~140μm, d_p (depth of diffusion)~2μm).

3. FEM analysis of dynamic behavior

A numerical simulation was performed for the structure of accelerometer by means of the COSMOS/M – GeoSTAR software attached to SolidWorks programming medium, using 9600 elements of 3D SOLID interconnected in 12573 nodes. The material properties of the component elements are given in table 1.

Table 1

Properties of the structure materials

Material	Si	SiO_2
Elastic modulus (GPa)	$B = 97.8$	$E = 70$
Poisson's ratio ν	0.28	0.17
Density ρ (kg/m^3)	2330	2200

For the silicon elastic modulus [13], Bulk modulus *(B)* was considered because, in a previous authors' research work [14], it was proved to be the most appropriate value with respect to the dynamic Young's modulus value experimentally determined on cantilever samples detached from the actual accelerometer structure. The resonant (natural) frequencies from the first to the

third vibration mode obtained by FEM are shown in Fig. 3. The frequencies are equal for similar modes of vibration (2-3) due to the symmetry As it was expected, the natural frequencies are high, in the range of kHz, because the oscillating mass is extremely small, associated with a relatively large stiffness.

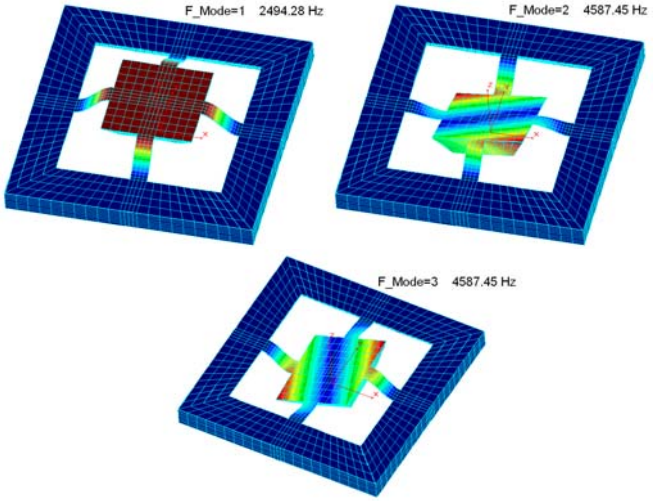

Fig. 3. The first three modes of the accelerometer.

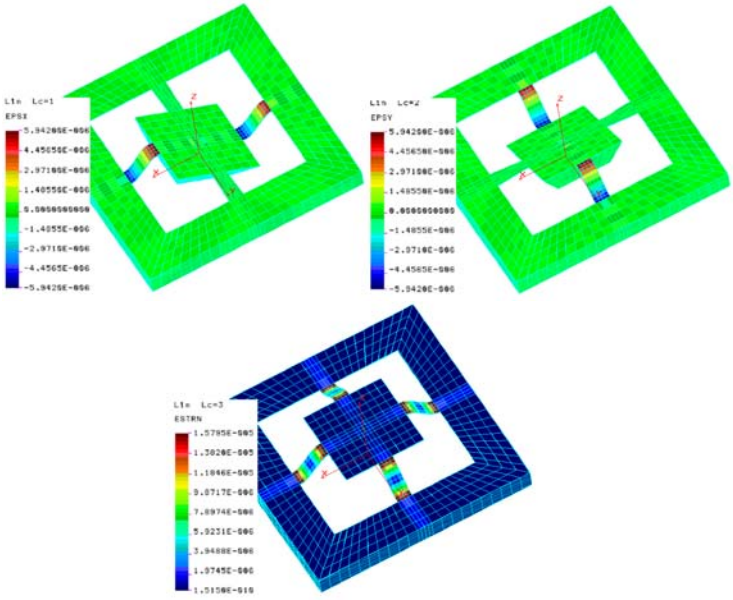

Fig. 4. Active area strains determined for an acceleration of 10 *g* applied on each axis ((for the Oz axis, resultant strains are shown).

From functional point of view, when a force is applied on the inertial mass, in sensor plane or normal direction, the micro-beams deflect (Fig. 4). The strains occurred in the active areas of the sensor (those in which the piezoresistors are diffused, at the interface Si-SiO_2) give the measure of the applied load by their conversion into electrical signals.

4. Piezoresistors location and sensitivity estimation

By combining the responses of eight piezoresistors located in adequate positions on micro-beams, nearly the rim and the inertial mass, the normal and/or lateral loads applied to the sensor can be determined.

It can be observed (figures 2 and 5a) that the resistors $R_1...R_4$ react to the forces directed along the Ox axis, while the resistors $R_5...R_8$ detect the forces acting along the Oy axis. Combinations of these resistors allow the normal forces sensing. More precisely, if a normal force (N) is applied on the sensor surface, piezoresistors R_2, R_3, R_6, R_7 will be subject to tensile (T)/compressive (C) stresses and, consequently, their electric resistance values will increase/decrease respectively. At the same time, the electric resistance values of the piezoresistors placed nearly the rim R_1, R_4, R_5, R_8 will have a contrary variation. If the force is laterally applied, in plane of sensor, the piezoresistors R_1, R_3, R_5, R_7 will be subjected to a tensile stress and their electric resistance will increase, while the piezoresistors R_2, R_4, R_6, R_8 will be subjected to a compressive stress and their electric resistance will decrease.

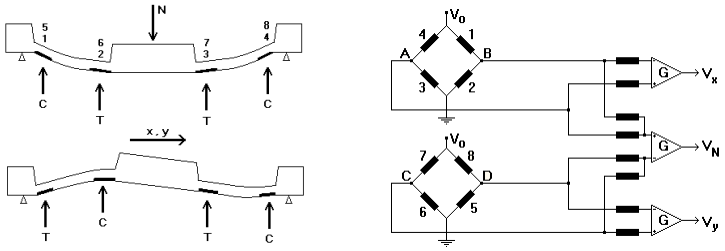

Fig. 5. Scheme of deflection of the piezoresistive accelerometer structure (a) and signal conditioning circuit scheme (b).

The piezoresistors connecting is made such that on each direction a Wheatstone bridge is obtained. The components of the resultant force which acts onto the sensor can be determined by an adequate design of the signal conditioning circuit, figure 5b: R – nominal value of the piezoresistor resistance; $\pm\Delta R/R$ – relative variation of the piezoresistance due to the tensile (T) / compressive (C) stress respectively; G – overall gain of the amplifier; V_o – bridge supplying voltage; V_X, V_Y and V_N – output voltages proportional to the

components of the resultant force acting onto the sensor. Through connection of the four piezoresistors placed on micro-beams found on the same symmetry axis in an Wheatstone bridge so that two piezoresistors from opposite arms are subjected to a tensile stress and the other two, from adjacent zones, to a compressive stress, both sensitivity increasing and decoupling of force components are occured (each bridge must give a proportional signal with the applied force on a certain direction without as the other components influence the output signal). The change in resistance of piezoresistors $\Delta R/R$ depends on the strains (at the interface Si-SiO_2, in the active areas where the piezoresistors are diffused) according to:

$$\Delta R / R = k_s \varepsilon_l , \tag{1}$$

where:

ε_l – longitudinal strain;

k_s – longitudinal gauge factor of piezoresistor, depending on type and concentration of dopant (resistivity) and crystalline direction of strain.

The longitudinal gauge factor of a piezoresistor embedded on the top surface of a silicon micro-beam pointing in the <110> direction, p-type doped (with boron), with resistivity of 7.8 Ω cm, may be computed as below [15].

The longitudinal piezoresistive coefficient is:

$$(\pi_{11} + \pi_{12} + \pi_{44})/2 = \frac{(6.6 - 1.1 + 138.1)\times 10^{-11}}{2} = 71.8 \times 10^{-11}\ \text{Pa}^{-1}. \tag{2}$$

Young's modulus of single-crystalline silicon is 168 GPa for <110> orientation. The effective gauge factor is:

$$k_s = 71.8 \times 10^{-11}\,(1/\text{Pa}) \times 168 \times 10^{9}\,(\text{Pa}) = 120.6 \ . \tag{3}$$

Considering figure 5, the output voltage variations as a result of microaccelerometer loading are [16]:

$$\Delta V_X = \frac{1}{4} k_s (\varepsilon_2 + \varepsilon_4 - \varepsilon_1 - \varepsilon_3) V_0 , \tag{4}$$

$$\Delta V_Y = \frac{1}{4} k_s (\varepsilon_5 + \varepsilon_7 - \varepsilon_6 - \varepsilon_8) V_0 , \tag{5}$$

$$\Delta V_Z = \frac{1}{8} k_s (\varepsilon_2 + \varepsilon_3 + \varepsilon_6 + \varepsilon_7 - \varepsilon_1 - \varepsilon_4 - \varepsilon_5 - \varepsilon_8) V_0 . \tag{6}$$

The sensitivity can be defined as the ratio between the output signal ($\Delta V_{x,y,z}$) and the supplying voltage (V_o):

$$S = \frac{\Delta V}{V_0} . \tag{7}$$

Based on FEM analysis (figure 4), strain variation and arrangement of piezoresistors along the Ox (similar to Oy due to the symmetry) and Oz axes were determined and are illustrated in Figs. 6 and 7.

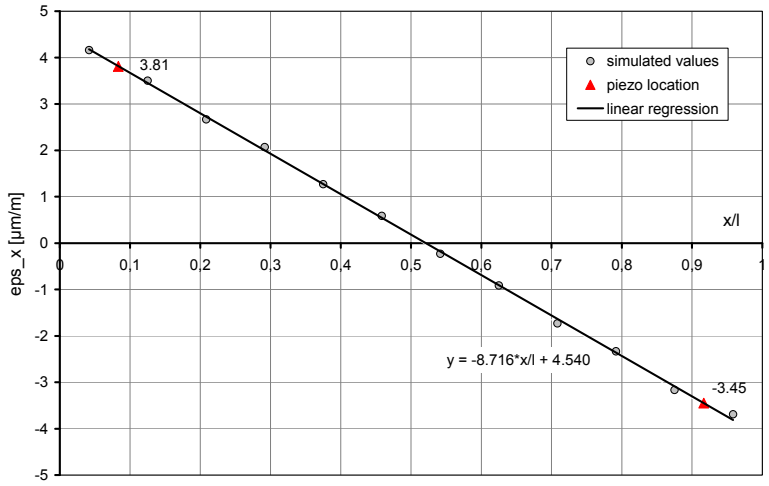

Fig. 6. Strain variation and piezoresistors location along the Ox oriented micro-beam.

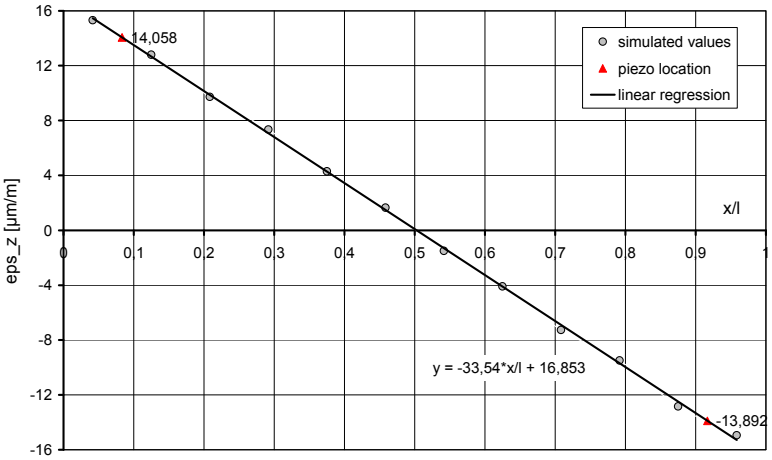

Fig. 7. Strain variation and piezoresistor location along the Oz oriented micro-beam.

The strain values, on longitudinal directions of piezoresistors, computed by FEM for three case of inertial force loading are given in table 2.

The values of sensor sensitivities on the three directions are as follows:

S_X = -0.0437 mV/V/g, S_Y = 0.0437 mV/V/g and S_Z = 0.1685 mV/V/g.

One can observe that the normal sensitivity of the sensor, corresponding to a normal direction loading, is 3.85 times higher than the lateral sensitivities and, also, effects decoupling of the acceleration components occurred.

Table 2

Strain values in longitudinal direction, at the interface Si-SiO_2

ε [μm/m]	Case 1 (Ox axis load) a_x=10 *g*	Case 2 (Oy axis load) a_y=10 *g*	Case 3 (Oz axis load) a_z=10 *g*
ε_1	3.45	Ox oriented micro-beams are subject to a torsional strain ε_t=0	-13.89
ε_2	-3.81		14.058
ε_3	3.81		14.058
ε_4	-3.45		-13.89
ε_5	Oy oriented micro-beams are subject to a torsional strain ε_t=0	3.45	-13.89
ε_6		-3.81	14.058
ε_7		3.81	14.058
ε_8		-3.45	-13.89

In Fig. 8, variation of sensitivities on X (Y) and Z directions as a function of micro-beam length / thickness ratio is represented. It could be useful for a pre-dimensioning of suspension arms of the accelerometer structure.

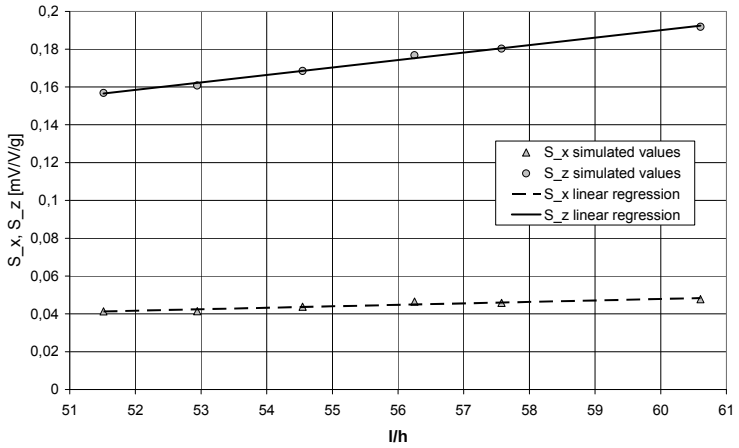

Fig. 8. Sensitivity variation with micro-beam length (l) / thickness (h) ratio.

5. Fabrication process

A combination of lithography-based bulk and surface structuring processes, carried out successively, was used for fabricating the silicon micromechanical device.

Wet (or liquid phase) anisotropic etching of silicon is one of the key technologies of silicon micromachining. It is also referred to as "bulk micromachining", because in this technology the body of the silicon wafer is etched away. Cantilever beams, diaphragms and other complicated 3D structures can be formed by this technique. In comparison with dry (or plasma phase)

etching, the inexpensive wet etching has been extensively employed for the fabrication of MEMS components based on single crystal silicon, especially on (100) wafer.

(100) Silicon wafers of 525 μm thickness were used in our experiments. The masking layer was 1800 Å thermal oxide, SiO_2. The etching solution was KOH 25 wt% at 80°C, with an etch rate of 1.25 μm/min. In absence of a stop etch layer, etching time was estimated to create the required height of the inertial mass. Alignment front to back of the masks relative to the wafer was used during the photolithographic processes. Partial des-oxidation only on the front side (50% HF: 40% NH_4F:H_2O, 35°C, 0.1 μm/min etch rate) was made in order to avoid the stress induced in the thin micro-beams by an oxide layer too thick.

The inertial mass is shaped like a truncated pyramid due to the anisotropic etching of silicon in KOH. Corner compensation [17] in the design of photo masks (Fig. 9) had to be used to achieve the shape of the mass.

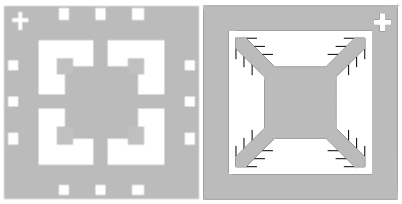

a) b)

Fig. 9. The front side (a) and the back side (b) mask configurations and compensation structures for inertial mass of the microaccelerometer.

Micro-photos of the microaccelerometer structure are shown in Fig. 10.

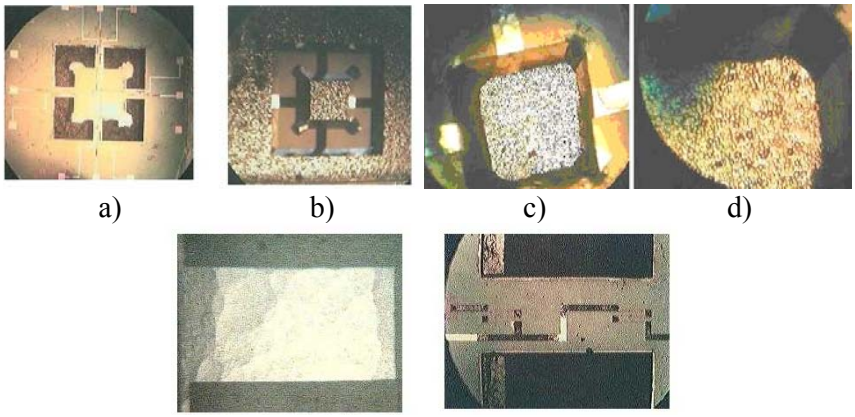

a) b) c) d)

e) f)

Fig. 10. Images viewed on an optical microscope of the bulk-micromachined accelerometer: a) – front side structure, b) – back side structure, c) – inertial mass, d) – a detailed corner of the inertial mass, e) – back side micro-beam, f) – front side micro-beam.

6. Vibration testing and results

In order to validate the FEM analysis results and to characterize the geometry and the dynamic behavior of performed structures, the MSA-500 Micro System Analyzer was used (Fig. 11). By using the LDV and WLI techniques, fast, real-time 3D analysis of out-of-plane structural vibration and surface topography, respectively, are provided [18].

The measurements were made on individual chips bonded through the structure rim onto a metal rigid plate of 12 x 12 x 5 mm^3. The plate was fixed through an elastic double adhesive layer on a piezoelectric excitator consisting of a multilayer ceramics piezoelectric actuator mounted in an elastic pre-tensioned housing. After measuring, significant differences between the similar modes of vibration 2-3 were found. These differences can be explained by different behavior of the four micro-beams because of the technological execution errors and the material anisotropy.

For the first three modes, the measured natural frequencies compared with those predicted using FEM analysis are given in table 3.

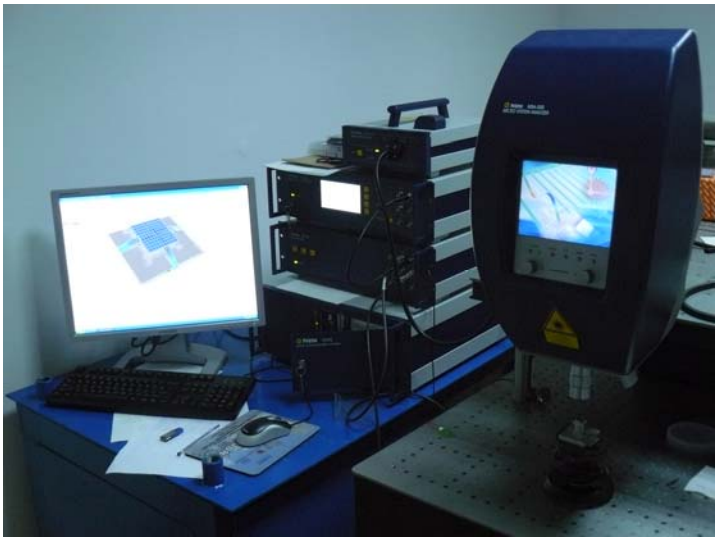

Fig. 11. The system of Polytec MSA-500, left (bottom to up): Data Management System, Vibrometer Controller , and Junction Box, right: Fiber-Optic Interferometer and Measurement Head. The tested structure can be viewed on the monitor screen.

Table 3

The experimental and FEM determined resonant (natural) frequencies

Mode no.	Experimental *f* (Hz)	FEM *f* (Hz)	Deviation (%)
1	2384.4	2494.3	**4.6**
2	4229.7; 4235.9	4587	6.7 (average value)
3	4837.5; 4835.9	4587	

7. Conclusions

The paper analyses FEM simulation aspects of performance characteristics (natural frequencies, piezoresistors location and sensitivity) of a MEMS operating out-of-plane accelerometer, with piezoresistive detection. As was expected, the natural frequencies are high, in the range of kHz, because the oscillating mass is extremely small, associated with a relatively large stiffness. As it was expected, the natural frequencies are high, in the range of kHz, because the oscillating mass is extremely small, associated with a relatively large stiffness. It was observed that the normal sensitivity of the sensor, corresponding to a normal direction loading, is 3.85 times higher than the lateral sensitivities. The effects decoupling of the acceleration components has been noticed (the output signal of each bridge is proportional with the bridge loading, and the other components do not influence the output signal).

The fabrication process of accelerometer structure by using MEMS technology (silicon bulk-micromachining) and vibration testing on the MSA-500 Micro System Analyzer are, also, presented. In absence of a stop etch layer, etching time was estimated to create the required height of the inertial mass. The etching time variation for releasing the accelerometer structure from the silicon wafer, as well as the tolerance for front-down side masks misregistration and misalignment have resulted in variations of thickness and length of the four suspension micro-beams, which were pointed out by measurements on MSA-500, when significant differences between the similar modes of vibration 2-3 were found. For all that a good agreement was found, the numerical model of computation has been experimentally validated with a precision of 4.6 %, for the first natural (fundamental) frequency. Bulk modulus *(B)* was used in simulation because, in a previous authors' research work, it was proved to be the most appropriate value with respect to the dynamic Young's modulus value experimentally determined on cantilever samples detached from the actual accelerometer structure under study.

Further research will continue to develop the numerical analysis by FEM in correlation with the experimental tests, considering the effect of the asymmetry of accelerometer structure induced by the execution errors (variation of micro-beam length and thickness) on the resonant frequencies and sensitivity. Because, at resonance, the suspension arms have great deformations, even though the acceleration at input is relatively low, layers of cover for amortization should be studied.

R E F E R E N C E S

[1] *M. Gad-el-Hak (ed.),* "Design and Fabrication, Ch. II - 16", in The MEMS Handbook, CRC Press, Boca Raton, FL, pp. 479 – 642, 2002

[2] *X. F. Zha,* "Database System for Design and Manufacturing of MEMS", in Int. Journal of Adv. Manuf. Technol., **vol. 32**, no. 3-4, 2007, pp. 378-392

[3] *C. Xue, S. Chen, H. Qiao, W. Zhang, J. Xiong, B. Zhang and G. Zhang,* "Development of a Novel Two Axis Piezoresistive Micro Accelerometer Based on Silicon", in Sensor Lett., **vol. 6**, no. 1, 2008, pp. 1-10

[4] *A. B. Joshi, B. P. Joshi, S. Sam Baskar, K. Natarajan and S. A. Gangal,* "Design and Fabrication of High Sensitive Piezoresistive MEMS Accelerometer", in Sensors & Transducers Journal, **vol. 91**, no. 4, 2008, pp. 76-83

[5] *Ranjith Amarasinghe, Dzung Viet Dao, Toshiyuki Toriyama and Susumu Sugiyama,* "Development of Miniaturized 6-Axis Accelerometer Utilizing Piezoresistive Sensing Elements", in Sensors and Actuators A, **vol. 134**, no. 2 , 2007, pp. 310-320

[6] *V. Ferrari, A. Ghisla, D. Marioli and A. Taroni,* "MEMS Accelerometer With Multiaxial Response by Dynamic Reconfiguration of Piezoresistive Bridges", in Proceedings of Eurosensors XX Conference, Göteborg, Sweden, Sept. 2006, M2B-P18

[7] *M. Zhu, P. Kirby and M. Y. Lim,* "Modelling of a Tri-axial Micro-Accelerometer with Piezoelectric Thin Film Sensing", in Proceedings of IEEE Sensor, Toronto, Canada, Oct. 2003, pp. 434-435

[8] *F. Zhang, X. He, Z. Shi and W. Zhou,* "Structure Design and Fabrication of Silicon Micro-accelerometer Based on Electrostatic Rigidity", in Proceedings of the World Congress on Engineering (WCE), London, U.K., July 2009, **vol. 1**, pp. 469-473

[9] *K. Petsch and T. Kaya,* "Design, Fabrication, and Analysis of Three-Direction Capacitive Accelerometer", in Proceedings of the 2012 ASEE North Central Section Conference, American Society for Engineering Education, pp. 1-16

[10] *Susan X. P. Su, H. S. Yang and Alice M. Agogino,* "A Resonant Accelerometer With Two-Stage Microleverage Mechanisms Fabricated by SOI-MEMS Technology", in IEEE Sensors Journal, **vol. 5**, no. 6, 2005, pp. 1214-1223

[11] *G. K. Fedder,* "Structured Design of Integrated MEMS", in MEMS '99, Proceedings of the 12th IEEE International Conference on MEMS, Jan. 1999, pp. 1-8

[12] *P. J. Saggal, C. Furlong and R. J. Pryputniewicz,* "Effects of the Proof Mass Suspension Mechanism on Sensing Ability of MEMS Accelerometers", in Proceedings of SEM Annual Conference & Exposition, 2003, s17p02

[13] *M. A. Hopcroft, W. D. Nix and T. W. Kenny,* "What is the Young's Modulus of Silicon?", in J. Microelectromech. S., **vol. 19**, no. 2, 2010, pp. 229-238

[14] *G. Ionascu, A. Sandu, L. Bogatu, C. D. Comeaga, E. Manea and D. Besnea,* "A Comparative Study of Computation Models for Dynamic Behaviour of MEMS Structures", in Proceedings of the 34th International Semiconductor Conference (CAS), Sinaia, Romania, Oct. 2011, **vol. 2**, pp. 395-398

[15] *W. Göpel, J. Hesse and J. N. Zemel (eds.),* "Piezoresistive Sensors", in Sensors, vol. 7, VHC Verlagsgesellschaft, Weinheim, Germany, 1994, pp.145 - 172

[16] *M. Sandu, A. Sandu, St. Sorohan and M. Gavan*, "Indrumar in Proiectarea senzorilor cu traductoare rezistive (Guideline in Designing Sensors with Resistive Transducers)", Printech, Bucuresti, 2005

[17] *A. Kociubiński, M. Duk, T. Bieniek and P. Janus,* "Modeling, Simulation and Calibration of Silicon Wet Etching", in Journal of Telecommunications and Information Technology, **vol. 4**, 2009, pp. 65-70

[18] *C. D. Comeaga and C. G. Alionte,* "Testing Methods for the Dynamics of Microstructures", in Proceedings of International Symposium AVMS'2009, Timisoara, Romania, May 2009, pp. 70-75.